Jpn. J. Appl. Phys. Vol. 38 (1999) pp. 1239–1242
Part 1, No. 2B, February 1999

Improvement of Internal Quantum Efficiency in 1.55 μm Laser Diodes with InGaP Electron Stopper Layer

Patrick ABRAHAM*, Joachim PIPREK, Steven P. DENBAARS and John E. BOWERS
Department of Electrical and Computer Engineering, University of California Santa Barbara, CA 93106, USA

(Received June 22, 1998; accepted for publication August 12, 1998)

This paper investigates the effect of the conduction band offset energy at the interface between the separate confinement layer (SCL) and the p-cladding on the temperature behavior of InGaAsP lasers emitting at 1.5 μm. The performance of a laser structure incorporating an additional $In_{0.81}Ga_{0.19}P$ barrier at that interface is compared to that of a regular laser structure. The results are analyzed using a comprehensive simulation software. It is shown that the current leakage at the SCL-p-cladding interface is not the dominant current loss mechanism at room temperature. However, at a higher temperature an additional InGaP electron stopper layer can efficiently reduce the electron leakage current. Finally, our measurements show that above a critical temperature the absorption loss increases dramatically.

KEYWORDS: long wavelength laser, electron leakage, InGaP, electron stopper layer, internal quantum efficiency, characteristic temperature, absorption loss

1. Introduction

There is strong evidence that the temperature sensitivity of the threshold current of long wavelength lasers is mainly controlled by Auger recombination.[1] However, the reason of the temperature sensitivity of the differential quantum efficiency (slope efficiency) is not as clear. For 1.3 μm lasers, loss outside the active region is important because the conduction band offset between the InP cladding layer and the separate confinement layer (SCL) is small.[2] Although this conduction band offset is not as small for 1.55 μm lasers, loss still has to be taken into account.

A typical solution to overcome that problem is to grow the structure in the InGaAlAs/InP system. It is then possible to take advantage of the type II interface between InP and $In_{0.52}Al_{0.48}As$ to introduce an electron barrier layer on the p-side using $In_{0.52}Al_{0.48}As$ and a hole barrier layer on the n side using InP.[3] However, in that case the difficulty is in the growth of Al containing alloys. The typical oxygen concentration in metalorganic vapor phase epitaxy (MOCVD) grown $In_{0.52}Al_{0.48}As$ is in the 10^{17} cm^{-3} to 10^{18} cm^{-3} range.[4] It produces deep n type levels that increase the internal absorption loss and the threshold current density. For 1.55 μm lasers the internal absorption loss and the threshold current density have been reported to be respectively as high as 27 cm^{-1} and 1.1 kA/cm^2 for 6 quantum wells (QW) GaInAlAs lasers (400 μm cavity length).[5] In the InGaAsP system for the same number of wells and the same cavity length these values are of the order of 10 cm^{-1} and 0.6 kA/cm^2 in our work. An intermediate approach, utilizing InGaAsP QW and InGaAlAs barriers with an $In_{0.52}Al_{0.48}As$ electron stopper layer has also been investigated.[6] In that case the internal absorption losses are again in the 20 cm^{-1} range, but the electron stopper layer was demonstrated to be efficient to decrease the leakage current. The use of an electron stopper barrier between the SCL and the QW has also been experimented. It also demonstrated to be efficient but in that case it is necessary to introduce p-doping in the electron stopper barrier to avoid any additional barrier for holes in the valence band.[7,8] The p-doping increases the threshold current by increasing the optical loss due to free carrier absorption and intervalence band absorption (IVBA) in the SCL where the confinement factor is important. For that type of structure to have no drawbacks, it would be necessary to use a material with a valence band energy in between that of the SCL material and that of the QW barrier. It was also proposed to use multiquantum barriers to create a virtual barrier on the p-side of the SCL. The advantage in that case is that the energy of the barrier introduced can be large and that it does not require the use of Al or p-doping of the SCL.[9] However, in that case it is also essential that the design of the barrier does not hinder hole injection in the active region.

To get further insight into the phenomena reducing the internal quantum efficiency at room temperature and higher temperatures we report in this paper on a simple modification of the classical InGaAsP laser structure increasing the electron confinement in the SCL. It consists of increasing the conduction band offset between the cladding layer and the SCL on the p-side. For that purpose, a thin $In_{0.81}Ga_{0.19}P$ layer is inserted between the p-InP-cladding layer and the SCL. The light hole band gap energy of $In_{0.81}Ga_{0.19}P$ coherently strained to InP is almost the same as that of InP but it has a type II interface with InP. The conduction band energy of $In_{0.81}Ga_{0.19}P$ is higher than that of InP. Hence, p-doping is not necessary in this layer in order to avoid any barrier for hole injection in the active region. The conduction band edge of $In_{0.81}Ga_{0.19}P$ is about 50 meV above that of InP at 4 K[10] and this can be estimated to be also valid at room temperature using the model-solid theory.[11]

Section 2 describes the structures with and without additional electron barrier layers (thereafter called respectively structures W and W/O). Section 3 describes how the absorption loss and internal quantum efficiency are measured and compares the experimental results achieved with structures W and W/O. These results are analyzed in §4 by simulations of both structures using an advanced laser software.[12]

2. Device Structures

The laser structures were grown in a MOCVD horizontal reactor made by Thomas Swan. The growth temperature and pressure were respectively 918 K (645°C) and 350 Torr. The sources were trimethylindium, trimethylgallium, tertiarybutylarsine and tertiarybutylphosphine.

*On leave from Laboratoire Multi-Matériaux et Interfaces, Université C. Bernard Lyon 1, France. E-mail address: abraham@opto.ucsb.edu

The active region of the laser structures consists of six 5.5-nm-wide 1%-compressive-strain QWs. The barriers are made of lattice matched 1.25 μm wavelength InGaAsP. The first and last barriers are 17 nm thick and those in between the QWs are 5.5 nm thick. On each side of the QW stack the SCLs are 100 nm thick and made of 1.15 μm wavelength InGaAsP. The photoluminescence wavelength of structures W and W/O is 1.5 μm. On the p-side of the structure, the first 130 nm of InP cladding layer next to the SCL was undoped to prevent back diffusion of Zn into the SCL. The thickness of the $In_{0.81}Ga_{0.19}P$ layer is 6 nm in structure W. Broad area lasers with 57 μm wide stripes were processed. The as-cleaved lasers were characterized under pulsed conditions (0.05% duty cycle) for temperatures ranging from 290 K (17°C) to 390 K (117°C).

3. Experimental Results

For a first order calculation, assuming the internal absorption loss α_i and internal quantum efficiency η_i to be constant above threshold and independent on the length of the cavity, the differential quantum efficiency η_d can be related to α_i and η_i by:

$$\frac{1}{\eta_d} = \frac{\langle \alpha_i \rangle}{\eta_i \ln\left(\frac{1}{R}\right)} L + \frac{1}{\eta_i} \tag{1}$$

where R is the mean reflection coefficient of the laser facets and L is the cavity length. Cavity lengths between 250 μm and 1 mm were utilized to measure α_i and η_i using eq. (1).

Table I compares the properties of structures W and W/O at 293 K (20°C). In addition to α_i and η_i, the threshold current densities per QW for 700-μm-long cavities J_{th} and for infinite cavity length $J_{th\infty}$, the transparency current density per QW J_{tr} and the modal gain at threshold per QW were also measured. The values reported here are characteristic of state of the art lasers. T_0 was calculated for 700-μm-long cavity lasers for temperatures ranging between 293 K (20°C) and 333 K (60°C). Although an improvement of the internal quantum efficiency η_i and of the T_0 of structure W could be expected, at room temperature they are comparable to those of structures W/O. All the other properties also show almost identical results. The largest differences are with the internal absorption losses and the threshold current densities that are respectively 15% and 14% higher in W than in W/O.

Table I. Comparison of results for the laser structures W/O and W at 293 K (20°C): η_i is the internal quantum efficiency, α_i the internal absorption loss, J_{th} and $J_{th\infty}$ the threshold current densities per QW for 700-μm-long cavities and for infinite cavity length, respectiveley, J_{tr} the transparency current density per QW and g_{th} the modal gain at threshold per QW. T_0, the characteristic temperature of the threshold current, was measured for temperatures between 293 K (20°C) and 333 K (60°C).

	Structure W/O	Structure W
η_i	0.69	0.67
$\alpha_i(cm^{-1})$	9.7	11.2
$J_{th}(A\,cm^{-2})$	73	83
$J_{th\infty}(A\,cm^{-2})$	56	61
$J_{tr}(A\,cm^{-2})$	45	48
$g_{th}(cm^{-1})$	8.3	8.2
$T_0(K)$	61	59

The way the differential quantum efficiency changes with respect to the temperature was also estimated using a characteristic temperature $T_{\eta d}$. The relation used for the fit is

$$\eta_d = \eta_{d0} \exp\left(-\frac{T}{T_{\eta d}}\right) \tag{2}$$

There is a critical temperature T_c that separates the two regions where I_{th} and η_d have different temperature dependencies.[13] Table II shows the values of the critical temperatures T_c and the characteristic temperatures T_0 and $T_{\eta d}$ above and below T_c for both structures for 250-μm-long lasers. The only clear difference between the two structures is with $T_{\eta d}$ below T_c. It increases from 113 K to 164 K on adding the $In_{0.81}Ga_{0.19}P$ electron barrier layer whereas above T_c the $T_{\eta d}$ values are about the same. On the contrary, the T_0's (below T_c) of structures W and W/O are close to each other.

The internal absorption losses α_i measured for laser structures W and W/O as a function of the temperature below T_c show very similar behavior. So, according to eq. (1) this means that the higher value of $T_{\eta d}$ for structure W is essentially due to the higher value of the characteristic temperature of the internal quantum efficiency $T_{\eta i}$ defined in the same way as $T_{\eta d}$ in expression (2). Indeed, Fig. 1 shows that the internal quantum efficiency of structure W/O decreases faster than that of structure W when the temperature increases.

For temperatures above T_c, the characteristic temperatures of structures W/O and W degrade strongly and are again the same. The two structures behave identically. This catastrophic degradation of InGaAsP long wavelength laser performance at high temperatures has been attributed to a pile-up of carriers, in particular holes, in the SCL.[13] At high temperatures, due to the small conduction band offset of this system (only 40% of the band gap energy difference is in the con-

Table II. Critical temperature T_c, characteristic temperature of the threshold current T_0 and of the differential quantum efficiency $T_{\eta d}$ below and above the critical temperature for 250-μm-long laser structures W and W/O

	Structure W/O		Structure W	
	$T_c \approx 370$ K		$T_c \approx 370$ K	
	$T < T_c$	$T > T_c$	$T < T_c$	$T > T_c$
$T_0(K)$	52	24	48	20
$T_{\eta d}(K)$	113	15	164	16

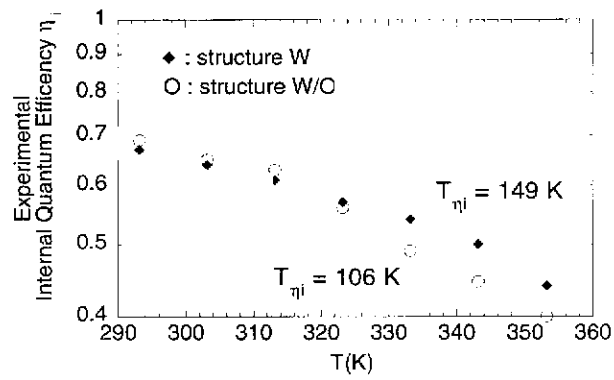

Fig. 1. Measured internal quantum efficiency of laser structures W and W/O as a function of temperature.

duction band offset) electrons leak out of the QWs into the SCLs. This produces an inbalance in the charge distribution between the QWs and the SCLs and creates an electric field that traps holes in the SCLs. The charge accumulation in the SCL significantly increases the internal absorption loss and recombination in the SCL that dominate and determine the temperature behavior at high temperatures.

Our observations are consistent with that explanation. First, the critical temperature is the same for structures W and W/O because it only depends on the conduction band offset between the QWs and the barriers. Second, a strong increase of the internal absorption loss accompanies the catastrophic degradation of the laser performance. In structure W/O the internal absorption loss at 363 K (90°C) is 17.4 cm^{-1}. This is a 64% increase compared to the absorption loss at 353 K (80°C) whereas the absorption loss increases only by 10 to 15% in the 293 K to 353 K (20°C to 80°C) range. Also, above T_c, the $T_{\eta d}$'s of structures W and W/O are again comparable because the electron barrier layer of structure W is outside the SCL and has no effect in preventing the pile-up of carriers in the SCL.

4. Analysis

An advanced laser simulation software[12] is used to analyze the effect of loss mechanisms on the temperature sensitivity of our laser diodes. The software calculates the optical gain in strained quantum wells based on the $4 \times 4\,\boldsymbol{kp}$ method including valence band mixing and carrier-carrier interaction. The computed photoluminescence spectrum as well as the gain peak wavelength agree well with our measured data. Multi quantum well (MQW) intervalenceband absorption (IVBA), Shockley-Read-Hall (SRH) recombination, spontaneous emission and Auger recombination are included in the calculations. The Auger coefficient was slightly adjusted to fit the measured threshold current of 118 mA at room temperature (laser W/O, length $L = 269\,\mu$m and width $w = 57\,\mu$m). Excellent agreement with the light versus current measurement is obtained at room temperature for structure W/O.

Calculations for structures W and W/O give the same threshold current and the same slope efficiency at room temperature. The magnitude of the SCL absorption is not changed automatically by the software with changing SCL carrier density. A constant value of $\alpha_{SCL} = 13.7\,cm^{-1}$ is assumed in all calculations. Since all other loss mechanisms are included, deviations from the measured threshold current can be related to changes of α_{SCL}. Due to the additional conduction band offset the InGaP layer introduces an additional resistance that requires the voltage across the structure to be slightly higher to get the same current. Compared to structure W/O this raises the Fermi level in the SCL and thus increases the carrier density and the absorption loss in the SCL. Some other additional effects may also contribute to the observed difference between the absorption loss of structure W and W/O.

The current calculation is based on a drift-diffusion model including thermionic emission at heterobarriers. Thermionic emission of electrons from the SCL can be identified as minority carrier current in the p-InP-cladding layer. The increment of this electron leakage current divided by the increment in total current above threshold leads to a leakage related differential efficiency η_{leak} that is found to be 98% in both devices at $T = 293$ K (20°C). Thus, leakage losses are quite small in our case and the InGaP stopper layer does not have a marked effect at room temperature.

This picture changes at higher temperatures. Figure 2 plots the calculated reduction of slope efficiency η_d, internal efficiency η_i, and leakage related efficiency η_{leak} for both devices. Up to $T = 333$ K (60°C), η_{leak} remains above 90% and the effect of the InGaP layer is negligible. But at $T = 353$ K (80°C), η_{leak} is strongly reduced, indicating escalating electron leakage due to the spreading of the Fermi distribution of electrons towards higher energies. Under these conditions, the InGaP layer starts to be beneficial in reducing electron losses. The leakage current reduction is visible in a plot of the electron current density of both structures (Fig. 3). Electrons are injected into the MQW from the n-InP on the left-hand side and mostly recombine within the MQW, but a small electron current remains on the right-hand-side in Fig. 3, indicating electron leakage into the p-InP cladding. With stopper layer, this leakage current is slightly reduced (solid line).

The slope efficiency η_d in Fig. 2 also decreases with higher temperature but not as strongly as that measured due to the constant absorption coefficient α_{SCL} in our calculation. In reality, α_{SCL} increases with higher temperature due to a higher SCL carrier density. In agreement with the experimental technique, the internal efficiency η_i in Fig. 2 is calculated from

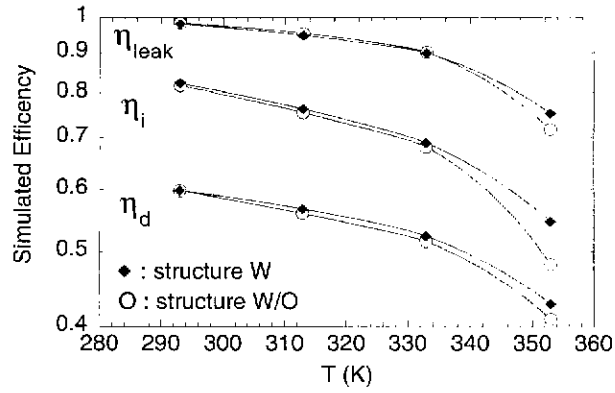

Fig. 2. Calculated external differential quantum efficiency, internal quantum efficiency, and leakage-related differential efficiency of structures W/O and W as a function of temperature.

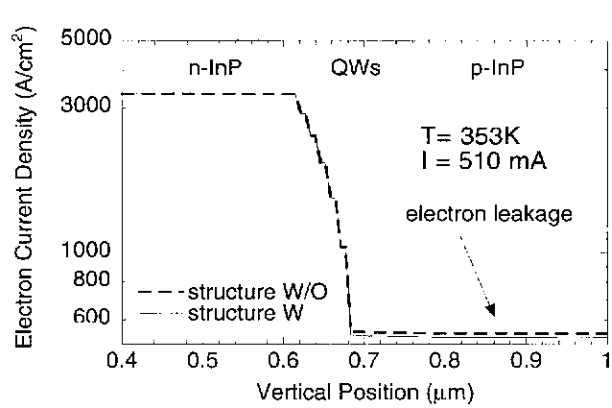

Fig. 3. Electron current density of structures W/O and W as a function of the vertical position in the laser structures.

simulations at different laser lengths using eq. (1). The computed values of $\eta_i(T)$ are within the standard deviation of the experiment (the plot $\eta_d^{-1}(L)$ results in different η_i if unreasonable η_d data are excluded). However, the $\eta_i(T)$ calculation clearly shows the measured impact of the InGaP layer at higher temperatures.

5. Conclusions

We proposed a simple way to increase the electron confinement in the SCL of long wavelength lasers by introducing an InGaP electron barrier layer on the p-side of the SCL. The comparison of the behavior of laser structures with and without the confinement layer shows that current leakage over the SCL-p-cladding interface is not the dominant carrier-loss mechanism at room temperature.

The effect of the InGaP stopper layer is to improve the internal quantum efficiency of the laser above 333 K (60°C) but below the critical temperature T_c of 370 K (97°C). However, it also slightly increases the carrier density in the SCL that increases the SCL absorption loss and the threshold current. Due to the small conduction band offset in the InGaAsP system, the band bending in the SCL above T_c produces a carrier pile-up that dramatically degrades the performance of the laser. In that regime the increase of the electron confinement in the SCL does not improve the behavior of the laser.

Acknowledgment

This work was supported by the Center for Multidisciplinary Optical Switching Technology (MOST), a DARPA-sponsored MURI (Multidisciplinary University Research Initiative).

1) E. P. O'Reilly, G. Jones, M. Silver and A. R. Adams: Phys. Status Solidi B **198** (1996) 363.
2) P. A. Andrekson, R. F. Kazarinov, N. A. Olson, T. Tanbun-Ek and R. A. Logan: IEEE J. Quantum Electron. **30** (1994) 219.
3) R. F. Kazarinov and G. L. Belenky: IEEE J. Quantum Electron. **31** (1995) 423.
4) T. Ohshima, H. Moriguchi, R. Shigemasa, S. Gotoh, M. Tsunotani and T. Kimura: Proc. 10th Int. Conf. Indium Phosphide and Related Materials, Tsukuba (Japan) 1998, p. 761.
5) B. Borchert, R. Gessner and B. Stegmüller: Jpn. J. Appl. Phys. **33** (1994) 1034.
6) H. Murai, Y. Matsui, Y. Ogawa and T. Kunii: Electron. Lett. **31** (1995) 2105
7) K. Takemasa, T. Munakata, M. Kabayashi, H. Wada and T. Kamijoh: Proc. 10th Int. Conf. Indium Phosphide and Related Materials, Tsukuba, 1998, p. 835.
8) A. Ubukata, J. Dong and K. Matsumoto: Proc. 10th Int. Conf. Indium Phosphide and Related Materials, Tsukuba, 1998, p. 721.
9) T. Loh, T. Miyamoto, F. Koyama and K. Iga: Jpn. J. Appl. Phys. **34** (1995) 1504.
10) A. Bensaada, J. T. Graham, J. L. Brebner, A. Chennouf, R. W. Cochrane, R. Leonelli and R. A. Masut: Appl. Phys. Lett. **64** (1993) 273.
11) C. G. Van de Walle and R. M. Martin: Phys. Rev. B **34** (1986) 5621.
12) PICS3D by Crosslight Software Inc.
13) S. Seki, H. Oohashi, T. Hirono and K. Yokoyama: IEEE J. Quantum Electron. **32** (1996) 1478.